CALCULATION OF THE DIMENSIONS OF ATTRACTORS FROM EXPERIMENTAL DATA

S. N. Lukashchuk, G. E. Fal'kovich, and A. I. Chernykh

UDC 532.517.3

Underlying the present-day approach to the problem of the onset of turbulence is the hypothesis that the phenomena determining the development of instability are finite-dimensional. Experimental data on the laminar turbulent transition [1, 2] support this standpoint, although rigorous mathematical formulation of this assertion, the theorem of the central manifold [3, 4], has been proven only for bifurcations of loss of stability by a stationary point. Intuitive arguments at present [5] suggest the probable existence of a finite set of excited degree of freedom, which determine the dynamics of the system over long times for more complex regimes of motion than the limit cycle.

In view of this, it is of considerable interest to determine the number of independent variables, which uniquely describe the potentially infinite-dimensional motion of a dissipative continuous medium, when the number of degrees of freedom, really set in motion, is not known beforehand. The necessary number of such variables is assigned by a one-to-one mapping of the phase space of asymptotic motion in Euclidean space, whose dimension will be called the dimension of embedding.

In this communication we propose a direct method of determining the dimension of embedding directly from experimental data, on the basis of an examination of the functional relation between the variables. Along with the embedding dimension we consider the scaling dimensions [6, 7] and the possibility of measuring them experimentally. The experimental data obtained in a study of the laminar-turbulent transition in circular Couette flow are analyzed in regard to dimension.

1. Dimension of Embedding. Suppose that for a dissipative dynamic system we measure the time dependence of a large number of different quantities $x_i(t)$, $i = 1, \ldots, N$. If the motion is finite-dimensional, the number of independent variables in $n_e$ and the first $n_e$ of the measured $x_i$ are in a one-to-one correspondence with the phase coordinates of the attractor, then any measured quantity $x_k$ when $k > n_e$ is a function (generally speaking, an unknown function) of the phase variables $x_1, \ldots, x_{n_e}$ and its evolution with time can be represented functionally in terms of the time dependence of the phase coordinates: $x_k(t) = f_k(x_1(t), \ldots, x_{n_e}(t))$. If for all k we verify whether or not there exists a functional dependence of $x_{k+1}(t)$ on the preceding k measurable quantities $x_1(t), \ldots, x_k(t)$, then clearly the functional dependence will appear for the first time at $k = n_e$, since the phase variables themselves are functionally independent. If the motion is infinite-dimensional, then such a functional dependence cannot appear at any k.

The geometric functional dependence is represented by a smooth surface in a (k + 1)-dimensional space. If $x_i^0$ is a point through which the phase curve passes at time $t_0$, then in the case of motion on an attractor in an infinitely long time the phase curve will return arbitrarily close to the point. We introduce a k-dimensional Euclidean metric $\rho_k(t, t_0) = \left[\sum_{i=1}^{k} (x_i(t) - x_i^0)^2\right]^{1/2}$. We take a sphere of radius ε with center at the point $x_i^0$. Suppose that d(ε) is the largest value $d(t, t_0) = |x_{k+1}(t) - x_{k+1}^0|$ for all points of the phase curve which fall inside this sphere in an infinitely long time. Then, with a smooth functional dependence for small ε we obtain small d(ε) and a constant C, such that the condition $d(\varepsilon) < C\varepsilon$ is satisfied, should exist. If there is no functional dependence, then $x_{k+1}(t)$ takes on values which do not depend on $x_i(t)$ ($i \leq k$) and, therefore, it is possible that $d(t, t_0) \neq 0$ even at $\rho_k = 0$. In this case $\lim_{\varepsilon \to \infty} d(\varepsilon) > 0$.

Novosibirsk. Translated from Zhurnal Prikladnoi Mekhaniki i Tekhnicheskoi Fiziki, No. 1, pp. 99-104, January-February, 1989. Original article submitted October 19, 1987.

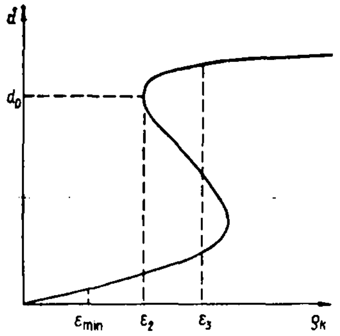


Fig. 1

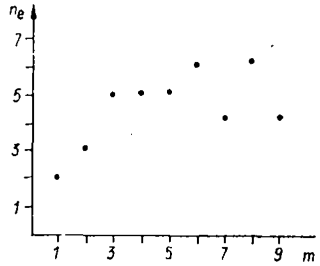


Fig. 2

The embedding criterion has a simple geometric interpretation. Let us project the phase curve onto the plane of variables $\rho(t, t_0)$, $d(t, t_0)$. Then $d(\varepsilon)$ as a function of $\varepsilon$ has the connotation of an envelope from above for that projection. In the case of embedding the envelope enters the point with coordinates (0, 0) with a nonzero slope. Otherwise, the envelope approaches the vertical axis with a nonzero value $d(0)$, which is commensurate with the dimensions of the attractor.

Let us consider the example of a phase trajectory, wound on a two-dimensional torus: $x_1 = (a + b\cos\varphi_2)\cos\varphi_1$, $x_2 = (a + b\cos\varphi_2)\sin\varphi_1$, and $x_3 = b\sin\varphi_2$ where $a > b > 0$. Suppose that the phase trajectory is specified by the equations $\varphi_1 = \omega_1 t$, $\varphi_2 = \omega_2 t$ with incommensurate $\omega_1$ and $\omega_2$. Locally the torus is two-dimensional, but the coordinates of a point on its surface $(\varphi_1, \varphi_2)$ are not determined uniquely by two Cartesian coordinates. This is because a straight line, which in the case of a general position pierce the torus at two points, corresponds to fixed values of the coordinates, e.g., $(x_1, x_2)$. If the functional dependence of the coordinate $x_3$ on $x_1$ and $x_2$ is verified by the proposed method, then in the two-dimensional $(\rho, d)$ plane $d(0)$ will be equal to the length of the segment intercepted by the piercing points on the straight line given by the equations $x_1 = x_1(t_0)$ and $x_2 = x_2(t_0)$. When any one of the three coordinates, taken with a delay, is verified for the functional dependence, we obtain $d(0) = 0$ and, therefore, the two-dimensional torus is embedded into the three-dimensional space.

If the phase trajectory is open, then in an infinitely long time its projection onto the $(\rho, d)$ plane everywhere densely fills the neighborhood of any point through which it passes. In this case there exist t such that the projection passes arbitrarily closely to the d axis and the envelope from above $d(\varepsilon)$ is defined correctly for any arbitrarily small $\varepsilon$.

In the experiment the measurements are made in a time $T_m$ at small but finite intervals $\Delta T$. As a result of the limitation on the finiteness of $T_m$, the $(\rho, d)$ plane is not filled densely everywhere. A line of finite length in the general case is embedded into three-dimensional space in the exact sense. Accordingly, when $k \geq 3$ there exists an $\varepsilon_p$ such that only that part of the phase curve which passes through the point $x^0$ at the time $t_0$ falls within the sphere $|x - x^0| = \varepsilon_p$.

All of this means that the passage to the limit as $\varepsilon \to 0$ is impossible and that the intermediate asymptotic form of $d(\varepsilon)$ must be determined in some range of scales $(\varepsilon_{min}, \varepsilon_{max})$. As $\varepsilon_{min}$ we should take a value which is several times the value of $\varepsilon_p$ averaged over the attractor. As for $\varepsilon_{max}$, the condition $\varepsilon_{min} \leq \varepsilon_{max} \leq R$ (R is the size of the attractor) should be satisfied.

Draw a straight line along the envelope $d(\varepsilon)$ by the method of least squares in this range of scales and extrapolating it to $\varepsilon = 0$, we obtain a new formulation of the embedding criterion. If the segment intersected on the d axis by the straight line is much smaller by modulus than the range of variation of d, then the embedding dimension has been reached.

We note that the choice of $\varepsilon_{max}$ becomes too subjective. Moreover, processing of experimental realizations showed that the envelope of the two-dimensional projection on the left and from above often has the form shown in Fig. 1 by the criterion just formulated, the attraction is embedded into the space, if we confine ourselves as much as possible to smaller scales and set $\varepsilon_{max} < \varepsilon_2$. There are several objections to this. First, as the realization increases in length, $\varepsilon_2$ can decrease and the criterion ceases to be satisfied. Second, it may be that on a sphere of radius $\varepsilon_2$ the function $x_{k+1}$, being a function of $x_i (i = 1, \ldots, k)$,

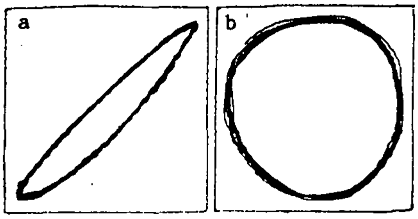

Fig. 3

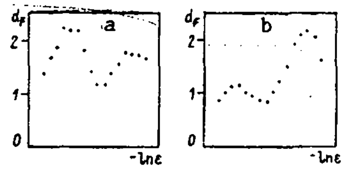

Fig. 4

is multiple-valued. Third, as a rule, $\varepsilon_2 \ll d_0$, where $d_0$ is comparable with the attractor dimensions, and the addition of $x_{k+1}$ as a new coordinate substantially increases the metric distance to those points to which it was slightly larger than $\varepsilon_2$, and $d \approx d_0$.

These concepts and observations give rise to a final form of the embedding criteria such that small scales are not mentioned at all. The dimension of the space was increased until the envelope became a single-valued function, emerging from zero and lying entirely below the straight line $d = C\rho_k$ (C is small). The estimate so obtained for the dimension of embedding may sometimes be too low. As is evident from the analysis carried out, however, this requires a detail study in each specific case.

2. Experiment. The dimension of the embedding and the scaling dimension with respect to nets [6, 7] was calculated for attractors of the laminar-turbulent transition in circular Couette–Taylor flow with a rotating internal cylinder. The measurements were made on a hydrodynamic stand, which was described in [8]. The diameter of the inner cylinder was $d_i$ = 35 mm. Liquid filled the gap, thickness $\Delta$ = 10 mm and height 280 mm, between the cylinders. For this geometry a configuration of 28 Taylor vortices and a flexural mode of the vortices, with six periods along the length of the neighborhood, correspond to the main state of flow. Using the electrodiffusion method [9], we measured the local shear stresses simultaneously at three different points on the inner surface of the immobile cylinder, corresponding to the boundaries of neighboring pairs of Taylor vortices. The measured signals were collected and processed with a computer.

The experiment was carrid out in the range 0.015 $Re_c$ to 1.05 $Re_c$, where $Re_c$ = 1030 is the critical Reynolds number for the formation of azimuthal waves ($Re = \omega d_i \Delta/2\nu$, $\omega$ is the angular velocity of the cylinder, and $\nu$ is the kinematic viscosity). A typical experimental realization consists of 64,000 or 128,000 points for each channel at a quantizing frequency of 16 Hz. The Reynolds number was maintained to within no worse than 0.15% during the measurements.

We used two methods to construct the phase space: the first coincided with the generally accepted [10-13] construction from one measured variable and in the second method the space was constructed from three measurable quantities, which were read at the same time, after which a shift by a constant interval T was made.

The phase space was constructed from slow envelops of signals, calculated by filtration at the frequency of oscillations of the azimuthal waves. A filtered envelope was an ensemble of 8000 points with a 1-second interval between points, which correspond to roughly 80 points in the characteristic period of a slow envelope. In constructing the phase space of high dimension, we took the time shift to be equal to 40 quantization intervals, i.e., roughly half of the period.

The series of rearrangements of the flow, which were observed in the experiment, was described in [9]. Below we examine regimes corresponding to two-dimensional tori and attractors following them. The numbers of the regimes m = 1, 2, 3, 4, 5, 6, 7, 8, and 9 correspond to Re = 1051.8, 1058.2, 1060.3, 1061, 1062.9, 1064, 1065, 1066, and 1066.8.

3. Calculation of the Dimension and Discussion of the Results. Figure 2 shows the dependence of the embedding dimension on the number of the experiment. The two-dimensional projection in the coordinates ($\rho_k$, d) was constructed for 15 points, uniformly distributed along the realization of the signal, and the results of their superposition on each other was shown on a graphic display. The superposition of several projections reduces the probability of the dimension being undervalued, since the solution for the embedding is determined by the worst of all the cases.

In relation to previously studied regimes it is known that m = 1 corresponds to the limit cycle, m = 2 corresponds to a resonance torus with 13/31 rotations, and m = 3 corresponds to a resonance torus with 3/7 rotations [9]. For m = 3 the embedding dimension $n_e = 4$, which is too much for a torus. This may be because the points at which the phase trajectory pierces the transversal plane do not lie on a closed curve homeomorphous with the neighborhood, as should be the case for a torus, but form a fairly diffuse cloud [9]. The diffusion may be due to both experimental noise and the fact that the attractor in fact is not a torus. As we see from Fig. 2, the number of variables sufficient for describing the flow remains small in the region of the laminar-turbulent transition. We should also note the nonmonotonic dependence of $n_e$ on Re, which indicates that the attractor may become more complicated or simpler as the nonlinearity increases.

Let us now discuss the results of measurements of the dimension from nets. In doing this we determine the number of points $N(\varepsilon)$ in the net of mesh $\varepsilon$ that covers the attractor. The dimension of the limit cycle should be one. Figure 3 shows the projection of the cycle onto the plane of the initial variables (a) and the plane of variables found by the time-series method (b). Figure 4 shows the dependence of the local slope $d_F$ of the curve of ln N versus ln $\varepsilon$, which was obtained by the method of nets in the range of scales from $2 \cdot 10^{-1}$ to $4 \cdot 10^{-2}$ for these two methods of constructing the phase space. The values of ln N were calculated for 20 values of $\varepsilon$ with different intervals on the logarithmic scale. The slope was determined by the method of least squares from three points. We see that only in case b was a segment with slope near 1 observed in the region of intermediate scales. The absence of such a segment in case a is due to the pronounced elongation of the cycle along the diagonal. Scales at which only one branch of the cycle passes through a square of area $\varepsilon^2$, but the noisiness of the trajectory does not have an effect, vanish because of this.

When m = 2, according to Fig. 2, three variables must be used. We assume the range of variation of signals for each variable to be equal to unity, whereupon the discretization step is such that the average distance between two successive points in time is of the order of $10^{-2}$. The range of $\varepsilon$ from $2 \cdot 10^{-1}$ to $2 \cdot 10^{-3}$ will be divided into 14 steps, which are uniform on the logarithmic scale. The dependence of the slope of the curve of ln N vs. $\ln(\varepsilon^{-1})$ is shown in Fig. 5. We see that at the first six points (i.e., in the range $\varepsilon = 2 \cdot 10^{-1}$–$3.8 \cdot 10^{-2}$) the dimension with respect to the nets is nearly 2. Calculating $d_F$ as the average over six points, we obtain $d_F = 2.07 \pm 0.04$. The error indicated here is the interpolation error, which can be calculated in the standard way (from the rms deviation). The accuracy of measurement of the hydrodynamic parameters from experiment is no worse than $10^{-3}$. We emphasize that with the indicated accuracy ($4 \cdot 10^{-2}$) we find, instead of the dimension from its literal topological definition (including the limit as $N \to \infty$, $\varepsilon \to 0$), the scaling index for a range of scales and a finite-dimensional set of points. The measurement of the dimension for m = 2 is consistent with the hypothesis in [9] that the attractor is two-dimensional. The numbers $d_F$ (are close to 2), which were obtained for m > 2, are considerably less reliable. This is because as the number k of variables used increases the error in the determination of $d_F$ increases approximately according to the law $\Delta d \sim e^{-1/d}$. This increase is due to the effective reduction of the number of points in the phase space for each of the k variables. For example, for m = 5 we have k = 3 and $d_F = 2.15 \pm 0.07$, k = 4 and $d_F = 2.14 \pm 0.14$, k = 5 and $d_F = 2.06 \pm 0.29$, and k = 6 and $d_F = 1.91 \pm 0.36$. From this it follows, in particular, that attempts to find a sufficient number of variables from the saturation of $d_F(k)$ involve considerable difficulties. For a more reliable measurement of the scaling dimensions it is necessary to increase the number of points in the initial realization, not by reducing the discretization step (on which d virtually does not depend) but by extending the observation time. This requires new experiments to be formulated.

It should be pointed out that since it is difficult to make an a priori estimate of the error contributed to the determination of the scaling dimensions by the finiteness and discreteness of the trajectory, with present-day experimental and computational capabilities it is scarcely meaningful to speak of measuring a fractional part of $d_F$. Measurement of positive Lyapunov exponents [12-18]. An an integer-valued quantity $d_F$ is an interesting characteristic of the dimension of the manifold into which an attractor can be mapped locally [6, 12, 18]. The embedding dimension (global characteristic) that we have proposed is equal to the dimension of Euclidean space, into which this manifold could be embedded without self-intersections. A regular procedure for constructing the minimum set of variables necessary for a local description of the attractor (local coordinates in the manifold) is lacking. It is important, therefore, to make an upper estimate of the number of variables of the general position which are necessary for describing the flow. This estimate is given by the embedding dimension $n_e$.

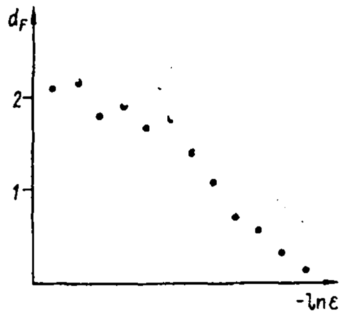


Fig. 5

Since the local nature of the embedding criterion has been discarded for calculating $n_e$, we must process a much smaller body of data than for determining the scaling dimensions. The altorithm for finding $n_e$ is simple, does not require a large volume of calculations, and is easily implemented on a computer.

Since the local nature of the embedding criterion has been dropped, the embedding dimension $n_e$, e.g., of a complex periodic trajectory, may be higher than three. The value of $n_e$, which is too high in comparison with the local criterion, can in this case be evidence of the complex arrangement of the cycle and the high probability that it will be transformed into a more complex regime of motion, no longer allowing a reduction of $n_e$, when the parameters of the system are disturbed.

The foregoing discussion permits a general conclusion to be made: determination of the embedding dimension should be the first step in the study of the finite-dimensional dynamics of a continuous medium or a finite-dimensional system with a very large number of degrees of freedom.

We thank V. S. L'vov and A. A. Predtechenskiĭ for their discussion of the work and E. A. Kuznetsov for a stimulating influence during the writing.

## LITERATURE CITED


1. M. I. Rabinovich, "Stochastic self-oscillations and turbulence," Usp. Fiz. Nauk., 125, No. 1 (1978).
2. J.-P. Echmann, "Roads to turbulence in dissipative dynamical systems," Rev. Mod. Phys., 53, 643 (1981).
3. J. Marsden and M. McCracken, Bifurcation of Creation of a Cycle and its Application [Russian translation], Mir, Moscow (1980).
4. V. I. Arnold, Supplementary Chapters of the Theory of Ordinary Differential Equations [Russian translation], Mir, Moscow (1978).
5. R. D. Richtmyer, Principles of Modern Mathematical Physics [Russian translation], Mir, Moscow (1984).
6. J. Farmer, E. Ott, and J. Yorke, "The dimension of chaotic attractors," Physica D, 7, 153 (1983).
7. S. N. Lukashchuk, A. A. Predtechenskiĭ, G. E. Fal'kovich, and A. I. Chernykh, "Calculation of the dimensions of attractors from experimental data," [in Russian], Preprint Inst. Avtomat. Elektrom., Sib. Otd., SSSR, Novosibirsk, No. 280 (1985).
8. V. S. L'vov, A. A. Predtechenskiĭ, and A. I. Chernykh, "Bifurcation and chaos in a system of Taylor vortices: a natural and numerical experiment," Zh. Éksp. Teor. Fiz., 80, No. 3 (1981).
9. S. N. Lukashchuk and A. A. Predtechenskiĭ, "Observation of resonance tori in the phase space of Couette flow," Dokl. Akad. Nauk SSSR, 274, No. 6 (1984).
10. N. Packard, J. Crutchfield, et al., "Geometry from a time series," Phys. Rev. Lett., 45, No. 9 (1980).
11. F. Takens, "Detecting strange attractors in turbulence," in: Lecture Notes in Mathematics, 898, Springer-Verlag, Berlin (1980).
12. A. Brandstater, J. Swift, et al., "Low-dimensional chaos in a hydrodynamic system," Phys. Rev. Lett., 51, No. 16 (1983).
13. A. Brandstater, J. Swift, H. Swinney, and A. Wolf, "A strange attractor in a Couette–Taylor experiment," in: Turbulent and Chaotic Phenomena in Fluids: Proceedings IUTAM Symposium, Kyoto, 1983, North-Holland, Amsterdam (1984).

14. B. Malraison, P. Atten, et al., "Dimensions of strange attractors. An experimental determination for the chaotic regime of two convective systems," J. Phys. Lett., 49, 897 (1983).
15. J. Roux, R. Simonyi, and H. Swinney, "Observation of the strange attractor," Physica D, 8, 257 (1983).
16. J. Guckenheimer and J. Buzyna, "Dimension measurements for geostrophic turbulence," Phys. Rev. Lett., 51, 1438 (1983).
17. M. Giglio, S. Musazzi, and S. Umberto, "Low-dimensionality turbulent convection," Phys. Rev. Lett., 53, 2402 (1984).
18. A. V. Gaponov-Grekhov, M. I. Rabinovich, and I. M. Starobinets, "Dynamic model of the spatial development of turbulence," Pis'ma Zh. Eksp. Teor. Fiz., 39, No. 12 (1984).